Initial State of an Enzymatic Reaction. Theoretical Prediction of Complex Formation in the Active Site of RNase T1

F. Cordes, E. B. Starikov, and W. Saenger*

Contribution from the Institut für Kristallographie, Freie Universität Berlin, Takustrasse 6, D-14195 Berlin, Germany

Received April 24, 1995[⊗]

Abstract: A computer model for the hydrated complex between the enzyme ribonuclease (RNase) T1 and its substrate guanylyl-3′,5′-guanosine has been refined using molecular dynamics simulation and quantum chemical calculations. Actual protonation states of the most important residues at the active site in the presence of the substrate were derived from published NMR titrations and pH-dependent kinetic studies, which were confirmed by independent Monte Carlo calculations (manuscript in preparation). The molecular dynamics trajectory has been analyzed to theoretically capture the initial point of the enzymatic reaction pathway. The changes in the charge distribution of the most relevant part of the enzyme−substrate complex have been checked by the CNDO/2-spd technique. The initial point of the enzymatic reaction pathway has been found to correspond, as expected, to the strained conformation of the "substrate + active site side chains" complex. His40, Glu58, Arg77, and His92 which are primarily involved in the enzymatic activity show hydrogen bond contacts to the substrate. In this scheme, Glu58 plays the role of general base and His92 acts as the general acid in the reaction pathway, while the other two residues stabilize the initial state of the reaction electrostatically.

Introduction

A variety of structural and functional studies have led to a general view on the mechanism of di-, oligo- and polyribonucleotide phosphodiester hydrolysis catalyzed by ribonucleases (RNases).[1−3] Because enzyme−substrate and enzyme−transition state complexes have very short lifetimes and thus cannot be captured by conventional experimental techniques, computer modeling is widely used to reconstruct the most salient features of the corresponding enzymatic reaction pathway.[4−7] Although much is known about the actual mechanism of RNase catalytic activity, details still remain a matter of debate.[3] First of all, prior to clarifying these details using methods for enzymatic activity simulations,[8−10] a plausible model for the initial state of the enzymatic reaction under study must be worked out in an independent way.

Specifically, the P−O5′ phosphoester bond hydrolysis catalyzed by RNases is known to be governed by a combination of "general base" and "general acid" residues in the active sites of these enzymes, and is recognized to proceed in two stages:[1−3] (a) transphosphorylation starting from dinucleoside-monophosphate monoanion and resulting in nucleoside-2′,3′-cyclophosphate monoanion formation; (b) hydrolysis starting from nucleoside-2′,3′-cyclophosphate and resulting in nucleoside-3′-monophosphate formation. For the pyrimidine-specific RNase A two histidines (protonated His119$^+$ and unprotonated His12) play the role of general acid and general base according to the conventional mechanism,[1] whereas in the guanine-specific RNase T1 the protonated His92$^+$ and the anionic Glu58$^-$ residues stand for the conventional choice of the general acid and general base, respectively.[2] Studies on the RNase T1-guided reaction kinetics[11,12] have indicated a residual activity upon genetic substitution of Glu58$^-$ to a neutral amino acid. The pH-dependent kinetics of these mutants[12] together with the knowledge of the orientation of His40 with respect to the ribose derived from X-ray structures of enzyme−inhibitor complexes[13−15] show that in this case the deprotonated His40 may become the general base in the RNase T1 active site, similar to His12 in RNase A. A proposal that His40 is essential for the reaction and may serve as the general base was also supported by the fact that His40Ala and His92Ala mutants show no activity, whereas the Glu58Ala[11,12] mutant possesses some residual activity. pH-dependent kinetic studies for wild-type RNase T1[12] showed that His40 is required to be protonated for optimal activity, and led to the conclusion that the protonated His40$^+$ must be directly involved in the electrostatic orientation of Glu58$^-$ and of the negatively charged substrate;[2,12] the actual role of this residue is not totally clarified at present.[3]

Another problem is connected with the preferential direction

* To whom correspondence should be addressed. FAX: +49 30 838 67 02.

⊗ Abstract published in *Advance ACS Abstracts*, October 1, 1995.

(1) Fersht, A. *Enzyme Structure and Mechanism*; W. H. Freeman: New York, 1985; 426−433.
(2) Heinemann, U.; Hahn, U. *Topics in molecular and structural biology: Protein nucleic acid interactions*; Saenger, W.; Heinemann, U., Eds.; 1989; Vol. 10, pp 111−141.
(3) Saenger, W. *Curr. Opin. Struct. Biol.* **1991**, *1*, 130−138.
(4) Holmes, R. R.; Dieters, J. A.; Galucci, J. C. *J. Am. Chem. Soc.* **1978**, *100*, 7393−7402.
(5) Balaji, P. V.; Saenger, W.; Rao, V. S. R. *J. Biomol. Struct. Dyn.* **1991**, *9*, 215−231.
(6) Deakyne, C. A.; Allen, L. C. *J. Am. Chem. Soc.* **1979**, *101*, 3951−3959.
(7) Haydock, K.; Lim, C.; Brünger, A. T.; Karplus, M. *J. Am. Chem. Soc.* **1990**, *112*, 3826−3831.
(8) Tapia, O.; Andres, J.; Safont, V. S. *J. Phys. Chem.* **1994**, *98*, 4821−4830.
(9) Lee, F. S.; Chu, Z. T.; Warshel, A. *J. Comput. Chem.* **1993**, *14*, 161−185.
(10) Tempszyk, A.; Tarnowka, M.; Liwo, A.; Borowski, E. *Eur. Biophys. J.* **1992**, *21*, 137−145.
(11) Nishikawa, S.; Morioka, H.; Kim, H. J.; Fuchimura, K.; Tanaka, T.; Uesugi, S.; Hakoshima, T.; Tomita, K.; Ohtsuka, E.; Ikehara, M. *Biochemistry* **1987**, *26*, 8620−8624.
(12) Steyaert, J.; Hallenga, K.; Wyns, L.; Stanssens, P. *Biochemistry* **1990**, *29*, 9064−9072.
(13) Heinemann, U.; Saenger, W. *Nature* **1982**, *299*, 27−31.
(14) Koepke, J.; Maslowska, M.; Heinemann, U.; Saenger, W. *J. Mol. Biol.* **1989**, *206*, 475−488.
(15) Heydenreich, A.; Koellner, G.; Choe, H. W.; Cordes, F.; Kisker, C.; Schindelin, H.; Adamiak, R.; Hahn, U.; Saenger, W. *Eur. J. Biochem.* **1993**, *218*, 1005−1012.

0002-7863/95/1517-10365$09.00/0

of the attack by the general acid on the target phosphate at the very beginning of the reaction. The conventional reaction mechanisms for RNases A and T1 predict first hydrogen bonding and then proton transfer from the general acid to the esteric O5′ oxygen of the target phosphate.[1-3] In the more recent mechanistic proposal by Anslyn and Breslow,[16] which is based upon kinetic studies on model systems, the general acid attacks the phosphate anionic oxygen instead. Although this mechanism has been criticized,[17] the phosphate anionic oxygen is highly attractive for the positively charged general acid. Such an opinion is supported by the results of molecular dynamics simulation on the RNase A−substrate complex,[7] which suggest that the general acid His119$^+$ is hydrogen-bonded to the phosphate anionic oxygen.

To capture the initial point of the enzymatic reaction pathway, we have represented a complete simulated molecular dynamics (MD) trajectory as alternating "walks near the local conformational minima" and "transitions between the neighboring conformational minima". We call the conformational minima in question "inherent structures", borrowing this notion and the corresponding computational algorithm from the molecular dynamics studies on liquid water (see, e.g., ref 18). According to the concepts about the general physicochemistry of enzymatic activity, the very beginning of the enzymatic reaction induces a strained conformation in the active site after binding the substrate which perturbs the equilibrium charge distribution in the system. The enzymatic reaction can be viewed as a sequential relaxation of the above nonequilibrium state toward the enzyme−product complex.[1] Bearing this in mind, we expect that the starting point of the enzymatic reaction pathway does not correspond to a conformation within the particular inherent structure, but to a transition state between two (or more) inherent structures. To qualitatively check whether the selected strained conformation provides the necessary redistribution of charge density in the "active site + substrate" complex, semiempirical (CNDO/2-spd) quantum-chemical estimations have been carried out.

Methods

MD Simulation. Our starting point is the complex between RNase T1 and guanylyl-3′,5′-guanosine (GpG) as proposed in ref 19 on the basis of the X-ray structure of the complex between RNase T1 and two guanosine molecules plus modeled SPC−water molecules[20] around the active site, followed by a short MD simulation with the GROMOS package.[21] The model is in general agreement with X-ray data of other complexes between RNase T1 and 2′,5′-GpG,[14] 3′-GMP,[15] 2′-AMP,[22] and two guanosines;[19] i.e., the general properties of the recognition site, catalytic site, and subsite are conserved (Figure 1).

This simulation was extended for a further 40 ps using the DISCOVER program[23] and the AMBER force field.[24] The parameters for the run are listed in Table 1. For the calculation of nonbonded interactions we used a cutoff distance of 14 Å, which was superimposed by a sigmoid "switch function" between 12 and 14 Å to avoid discontinuities during the MD integration. The simulation was performed at pH 6.0, the pH optimum of the RNase T1 enzymatic activity.[12] The pK values of the titrable side chains were approximated by the values of the corresponding moieties in solution. The pK values of the important side chains in the active site, His40 and His92, are known from NMR titrations for the wild-type enzyme to be greater than 7.5.[12,25,26] They even increase to values greater than 8.0 if the complex between RNase T1 and 3′-GMP is formed.[25] Moreover, His40 is expected from pH-dependent kinetic studies to be protonated for optimal activity,[12] and therefore only the deprotonated Glu58$^-$ can serve as the general base which is in accordance with the conventional mechanism.[3] Thus, we set all glutamic and aspartic acids as well as the substrate to be negatively charged and all lysines, arginines, and histidines to be positively charged. The total charge of the complex was −6.

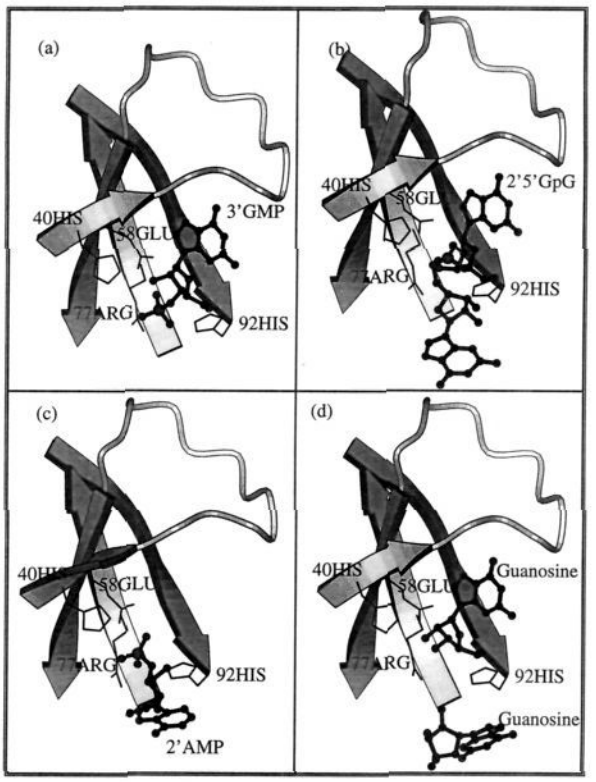

Figure 1. Conformation of the active site of RNase T1 in a complex with (a) 3′-GMP,[15] (b) 2′5′-GpG,[14] (c) 2′-AMP,[22] and (d) two guanosines.[19]

Table 1. MD Protocol

input	molecule	1468 enzyme atoms, 67 substrate atoms
	solvent	668 water molecules in a 20 Å sphere around phosphorus of the substrate
	force field	AMBER, all atom model
physical conditions	boundary	protein + water in a vacuum
	dielectric	$\epsilon = 1.0 \times$ (distance between charges)
	temperature	298 K
	volume	constant
	restraints	positions of water molecules in outer coordination shell
simulation conditions	time step	0.001 ps
	R cut	12−14 Å
	R switch	2 Å
equilibration	EM	500 cycles of steepest descent, 3000 cycles of conjugate gradient, stopped at a minimal gradient of 0.01 kcal/(mol Å)
	MD	5000 cycles = 5 ps
output	total time	40 ps
	coordinates	every 0.05 ps

(16) Anslyn, E.; Breslow, R. J. *J. Am. Chem. Soc.* **1989**, *111*, 4473−4482.
(17) Menger, F. M. *J. Org. Chem.* **1991**, *56*, 6251−6252.
(18) Ohmine, I.; Sasai, M. Prog. *Theor. Phys. Suppl.* **1991**, *103*, 61−78.
(19) Lenz, A.; Cordes, F.; Heinemann, U.; Saenger, W. *J. Biol. Chem.* **1991**, *266*, 7661−7667.
(20) Postma, J. P. M. Ph.D. Thesis, University of Groningen, 1985.
(21) Berendsen, H. J. C.; van Gunsteren, W. F. *GROMOS User's Manual*; University of Groningen: Groningen, The Netherlands, 1988.
(22) Ding, J.; Koellner, G.; Grunert, H. P.; Saenger, W. *J. Biol. Chem.* **1991**, *266*, 15128−15134.
(23) Biosym Technologies. *Discover User Guide, version 2.8.0*; San Diego, 1992.
(24) Weiner, S. J.; Kollman, P. A.; Nguyen, D. T.; Case, D. A. *J. Comput. Chem.* **1986**, *7*, 230−255.
(25) Arata, Y.; Kimura, S.; Matsuo, H.; Narita, K. *Biochemistry* **1979**, *18*, 18−24.
(26) Inagaki, F.; Shimada, K.; Miyazawa, T. *Biochemistry* **1985**, *24*, 1013−1020.

For further justification of this charge distribution, we performed with a novel method independent Monte Carlo simulations (manuscript in preparation) on the modeled enzyme substrate complex,[19] in which we allowed His40, Glu58, and His92 to change their protonation states at pH 6.0. The results show Glu58 in the role of general base according to the averaged charged state and vicinity to the 2′-hydroxyl group of the substrate, whereas the two histidines appear with a higher probability in the protonated than the deprotonated form. These results are consistent with the pK measurements[12,25] and our choice of protonation states.

The molecular dynamics trajectory has been analyzed on the basis of inherent structures.[18] The very beginning of every enzymatic reaction is believed to be connected with an onset of a local strain due to substrate binding: the active site of the enzyme "squeezes" the substrate molecule. This leads to a charge density redistribution in such a complex and initiates the enzymatic reaction (see, e.g., ref 1). Therefore, we classify the molecular dynamics trajectory of the enzyme−substrate complex into inherent structures and "conformational transition states" (CTSs) between the inherent structures. Both kinds of conformational states should be checked for necessary charge density redistribution, which they induce in the active site and in the substrate, using semiempirical quantum chemistry. To recognize the catalytically active CTS, the contacts between the side chain residues of the active site and the substrate functional groups must be in accordance with the known mechanistic proposals concerning the enzymatic reaction in question. In the search for initial states of the enzymatic reaction, (i) we have chosen only those "RNase T1 + substrate" conformations which contain the substrate + active site contacts according to the known mechanistic proposals about the RNase T1-guided phosphodiester hydrolysis,[2,3] (ii) we have carried out molecular mechanics minimization for every chosen RNase T1 + substrate conformation (see Table 1 for parameters) to arrive at the next local minimum on the energy hypersurface according to the "quenching" algorithm,[18] (iii) we have classified the energy-minimized structures thus revealed by means of principal component analysis (see, e.g., ref 27) into a few families which we called inherent structures,[18] and (iv) we have searched for transition states between the inherent structures, which can serve as initial states of the enzymatic reaction according to quantum-chemical calculations on the most interesting part of the catalytic site.

Principal Component Analysis. The principal component analysis[27] allows "families" of structures, the so-called inherent structures, to be reconstructed using a formal criterion of similarity between any two conformations in the set of energy-minimized structures. The number of inherent structures thus revealed will be much less than the initial number of "quenched" structures. The criterion of similarity between two macromolecular structures, a and b, is determined as the RMS (root mean square) difference between all interatomic distances of both structures. The RMS values were normalized to range from 0 to 1 according to the maximal value, RMS_{max}, of the matrix

$$\mathbf{RMS}(a,b) = \left[\frac{1}{N_{ij}(N_{ij}-1)}\sum_{i=1}^{N_{ij}}(r(a)_{ij} - r(b)_{ij})^2\right]^{1/2}$$

where N_{ij} designates the number of intramolecular distances r_{ij} between the atoms i and j of the structures a and b. The algorithm of the principal component analysis is presented in two steps: First, we have constructed the **RMS** matrix of generalized "distances" between the selected conformations of the enzyme−substrate complex, and second, we have solved the eigenvalue and eigenvector problem for this matrix. The number of eigenvalues greater or equal than unity represents then the number of inherent structures (actual potential energy minima), whereas the corresponding eigenvectors show the relationship between the inherent structures and all the quenched structures initially involved.

The eigenvector elements close to unity (practically greater than 0.8) show that the corresponding energy-minimized structure equals an inherent structure and those which are close to zero (practically less than 0.2) indicate no membership, whereas the eigenvector elements less than 0.8 and greater than 0.2 show "partial membership" in the inherent structure. If some energy-minimized structure partially belongs to more than one inherent structure, one could speak of a transition state (CTS) between two (or more) local minima.

(27) Reyment, R. A.; Jöreskog, K. G. *Applied factor analysis in the natural sciences*; Cambridge University Press: Cambridge, 1993.

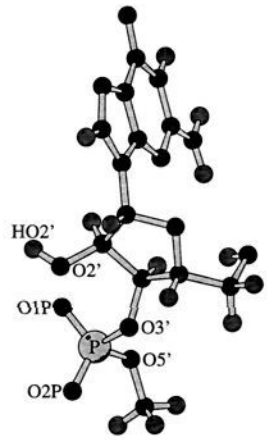

Figure 2. The "substrate" $GpCH_3^-$ used in the quantum-chemical calculations.

Semiempirical Quantum-Chemical Calculations. Since the main interest in the present study is the initiation of phosphodiester hydrolysis catalyzed by RNase T1, we have calculated Mulliken atomic partial charges and Wiberg indices (bond orders) for each of the inherent structures, as well as for each of the CTSs, which were obtained from analysis of the molecular dynamics trajectory. The atomic positions used in the quantum-chemical calculations were selected after the principal component analysis only for the most typical representative of each of the conformational families. The method is CNDO/2 (spd basis set), which explicitly takes into account the virtual 3d orbitals on the phosphorus. We believe that, for purely qualitative purposes, it makes practically no difference whether the CNDO/2-sp or the CNDO/2-spd technique is used. The earlier work[6] used the CNDO/2-sp approach without explicit 3d orbitals on the phosphorus to clarify qualitative aspects of the RNase A enzymatic activity and reported correlations to the results of ab initio techniques for the model phosphates. Another study[28] has revealed a tight correlation between the mononucleotide charge distributions obtained by CNDO/2-spd and by direct processing of the high-resolution X-ray data.

Since the 3′-terminal guanosine in the GpG substrate is irrelevant to the enzymatic recognition and reaction under study, it has been substituted by a methyl group; i.e., from here on, the monoanion $GpCH_3^-$ will be considered instead of the initial GpG− (Figure 2). The general acid $His92^+$ (as well as $His40^+$) has been mimicked in our calculations by the protonated imidazole ring plus a methyl group replacing the peptide backbone fragment. The $Glu58^-$ residue has been represented simply by the acetyl group, and the $Arg77^+$ side chain by guanidinium.

Results

The statistical investigation of the 40 ps MD trajectory with respect to specific hydrogen bonds between enzyme and substrate (i in the Methods) shows a permanent bond between His92 Nϵ2 and the anionic oxygen of the phosphate group, and in addition for some structures a weaker bond between the same Nϵ2 and the esteric oxygen O5′ (Table 2). Moreover, the statistics show that during a longer period of the dynamics $His40^+$ stabilizes via hydrogen bonds $Glu58^-$, and forms also a hydrogen bond to the O2′ of the substrate, which is expected to deprotonate in the first step of the conventional mechanism. For only a few structures (occurrence <1%) of the trajectory, $Glu58^-$, the only side chain which can play the role of the general base in this charge distribution, forms a hydrogen bond with O2′ of the substrate.

Because conformations with the same hydrogen bond pattern will probably be redundant for the analysis of the trajectory,

(28) Starikov, E. B.; Pedash, Yu. F. *Biopolymers* **1990**, *30*, 349−355.

Table 2. Statistics of Hydrogen Bonds at the Catalytic Site of the Enzyme[a]

donor	acceptor	% occurrence
His92 Nϵ2	Gua1 O1P	100.00
His92 Nϵ2	Gua1 O5′	4.74
Gua1 O2′	Glu58 Oϵ1	0.75
Gua1 O2′	Glu58 Oϵ2	0.26
His40 Nϵ2	Glu58 Oϵ2	99.63
His40 Nϵ2	Gua1 O2′	71.04

[a] Evaluation from 800 structures of the MD trajectory. Gua1 denotes the guanosine plus phosphate group at the recognition and catalytic site, whereas Gua2 designates the guanosine at the subsite.

we neglected the His92 Nϵ2···O1P and the His40 Nϵ2···O2′ bonds from explicit consideration, because they are found in all or nearly all conformations. From the structures with a His40 Nϵ2···Glu58 Oϵ2 hydrogen bond we selected only the one with the highest hydrogen bond energy.

Going forward with step ii for the search of an initial state of the reaction, Figure 3a shows the total energy of the remaining and minimized 47 structures, which are listed in chronological order. We notice that the first 15 structures still may not belong to the equilibrated regime of the trajectory. This corresponds to the appearance of dark regions in the **RMS**(a,b) matrix (Figure 3b), which indicates the growth of clusters with increasing time. The classification of the **RMS**(a,b) matrix leads to seven families of inherent structures corresponding to seven eigenvectors of the matrix with eigenvalues greater than or equal to unity (Figure 3d) (step iii in the Methods). "Full membership" is indicated by a black bar, while "no membership" is indicated by a white bar. Between these limits all gray bars represent partial membership. The classification shows only for a few structures full membership to one of the seven inherent structures; all other conformations can be described as transition states in the propagation of dynamics, which connect the inherent structures with each other.

The last step in the search for initial states of the reaction (iv in the Methods) was to analyze the energy of the substrate for all 47 structures (Figure 3c) and to pick up those for quantum-chemical analysis which belong to possible CTSs with high substrate energy. The most interesting of the CTSs is structure number 19, which possesses the highest substrate energy according to Figure 3c. From here on we shall refer to this CTS as an active CTS (ACTS). We should mention here that the idea of inherent structures and conformational transition states (CTS, ACTS) is comparable to the notion ES and ES‡, describing the ground and transition states of the enzyme–substrate complex within the catalytic reaction. We have chosen a different notation, because the investigated set of conformations generated by MD is limited to the situation before the chemical reaction starts.

The comparison of partial charges and Wiberg indices with the precessor and successor of the inherent structures in the course of the MD trajectory, numbers 6 and 3 (Table 3), shows that the polarization of the important O2′–HO2′ bond within the ACTS is much stronger compared with the results for the inherent structures 6 and 3.

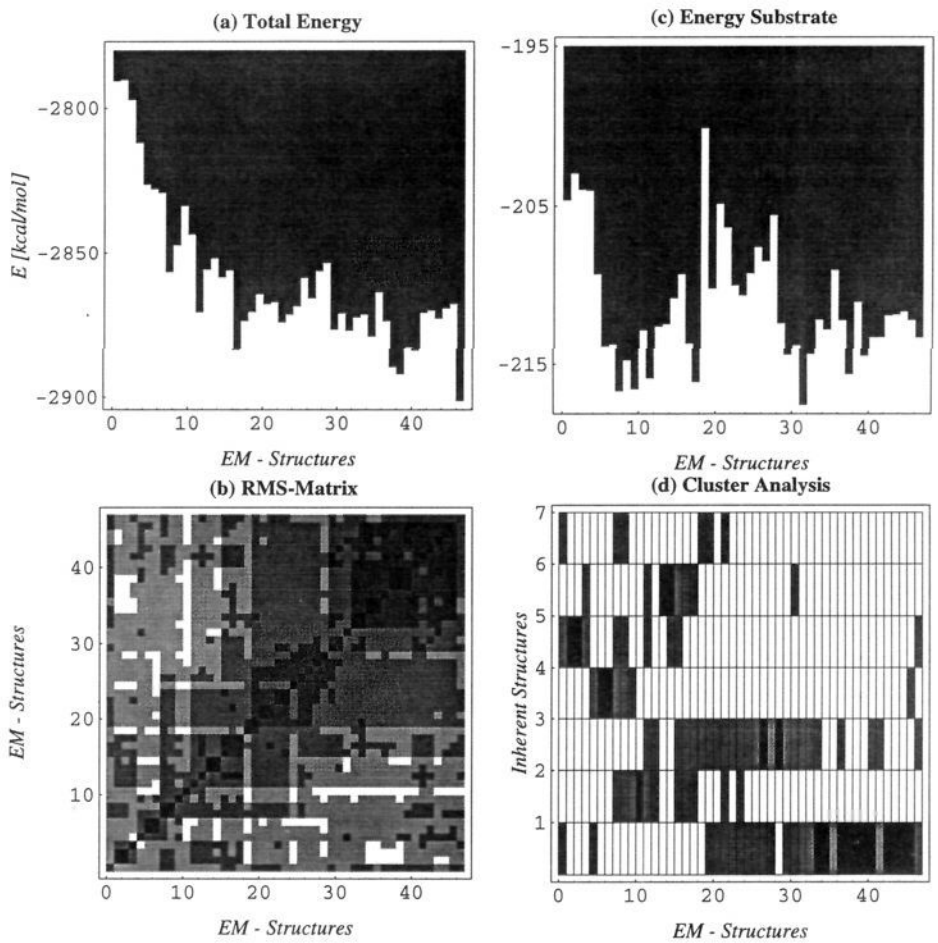

Figure 3. (a) Total energy of 47 selected structures from the MD trajectory after energy minimization. (b) **RMS**(a,b) matrix from the comparison of all 47 structures with each other; dark fields indicate high similarity. (c) Energy of the substrate in all 47 structures. (d) Analysis of principal components in the **RMS**(a,b) matrix; black, gray and white fields indicate full, partial, and no membership to one of the inherent structures.

Table 3. Results of the CNDO/2 Calculations with the spd Basis Set for the Substrate $GpCH_3$ in a Vacuum and in a Complex with the Reduced Side Chains of His40, Glu58, und His92 within the Functionally Active Conformational Transition State (ACTS) and the Two Adjacent Inherent Structures (Nos. 6 and 3).

	specific partial charges of the structures					
	no. 6		ACTS		no. 3	
atom	vacuum	complex	vacuum	complex	vacuum	complex
O2′	−0.315	−0.326	−0.240	−0.303	−0.313	−0.324
HO2′	0.218	0.203	0.141	0.194	0.218	0.205
O3′	−0.308	−0.286	−0.300	−0.280	−0.306	−0.285
P	0.439	0.492	0.426	0.490	0.439	0.498
O1P	−0.437	−0.484	−0.456	−0.499	−0.435	−0.482
O2P	−0.443	−0.440	−0.412	−0.420	−0.445	−0.445
O5′	−0.277	−0.290	−0.285	−0.296	−0.278	−0.288

	specific Wiberg indices of the structures					
	no. 6		ACTS		no. 3	
bond	vacuum	complex	vacuum	complex	vacuum	complex
O2′−H2′	0.889	0.903	0.962	0.910	0.892	0.904
P−O3′	1.041	1.138	1.025	1.131	1.045	1.142
P−O1′	2.058	1.932	2.045	1.917	2.062	1.936
P−O2P	2.000	1.949	2.074	2.005	1.999	1.943
P−O5′	1.103	1.141	1.080	1.120	1.098	1.140

	energy differences of the complex structures relative to ACTS (kcal/mol)		
	no. 6	ACTS	no. 3
energy	16.3	0.0	18.8

The Wiberg index for this bond decreases in the transition state due to complexation in contradiction to an increase in the inherent structures 6 and 3. As another consequence of complexation we find a higher polarization of the anionic oxygen O1P and a lower one for O2P. The CNDO/2 relative energies listed in Table 3 should be considered only as qualitative estimates, but in no way as an exact evaluation.

To investigate the sources which force the substrate into the transition state, we have compared the hydrogen bonds formed between substrate and RNase T1 in the ACTS and in the two structures 6 and 3 (Table 4). The main difference between ACTS and the inherent structures is the formation of a hydrogen bond between O2′ of the substrate and the anionic oxygen Glu58 Oϵ2 of the enzyme. This formation of an intermolecular hydrogen bond follows after the breaking of the internal hydrogen bond between O2′ and O2P of the substrate and is accompanied by the formation of a hydrogen bond between water molecule 629 and the O3′ of the ribose.

A detailed analysis of the energies in Figure 3a,c, which is concentrated on the inherent structures 6 and 3 and the quantum chemically interesting ACTS, confirms the significant increase

Table 4. Comparison of Hydrogen Bonds at the Catalytic Site between Inherent Structures 6 and 3 and the ACTS[a]

		D···A distance (Å) + D−H···A angle (deg)					
		no. 6		ACTS		no. 3	
donor	acceptor						
Tyr38 Oη	Gua1 O2P	2.6	174.2	2.6	168.7	2.6	173.3
His40 N	Glu58 O					3.5	147.4
Glu58 N	His40 O	3.2	157.4	3.0	158.8	2.9	162.3
His40 Nϵ2	Glu58 Oϵ2	2.6	139.2	2.7	141.9	2.6	135.5
His40 Nϵ2	Gua1 O2′	2.9	117.0	3.0	134.3	2.8	122.8
Arg77 Nϵ	Glu58 Oϵ1	2.7	162.7	2.7	158.5	2.7	152.4
Arg77 Nη2	Gua1 O2P	2.6	154.8	2.6	156.0	2.6	160.0
Arg77 Nη2	Gua2 O3′	2.8	167.0	2.8	157.0	2.8	164.0
His92 Nϵ2	Gua1 O1P	2.6	155.7	2.6	153.8	2.6	160.9
Asn98 Nδ2	Gua1 O1P	2.7	174.2	2.7	167.1	2.7	177.8
Gua1 O2′	Glu58 Oϵ2			2.6	139.9		
Gua1 O2′	Gua1 O2P	2.6	160.4			2.6	158.5
Water Molecules at the Catalytic Site							
Sol325 OW	Gua1 O2′	2.7	152.3	2.7	174.7	2.7	161.5
Sol629 OW	Gua1 O3′			2.9	128.9		
Sol381 OW	*Sol325 OW*	2.7	*173.6*	2.7	*174.5*	2.7	*173.7*
Sol629 OW	Sol381 OW	2.7	151.2	2.6	136.3	2.7	150.5

[a] Maximal donor−acceptor distance 3.5 Å, minimal D−H···A angle 115°. Gua2 denotes the guanosine at the subsite.

in substrate energy accompanied by a decrease in enzyme energy (Figure 4a,b). The results for inherent structure number 5 can be neglected, because it belongs to the nonequilibrated regime of the trajectory (see Figure 3a). The stacked bar chart picture, which distinguishes between different energy contributions, makes clear that the change in energy comes from nonbonded interactions, to which hydrogen bonds are included in the AMBER force field. A contribution from three water molecules around the catalytic site to the higher substrate energy in the ACTS can be neglected (Figure 4c), because the sum of the water energies is not extremal for the transition state. Nevertheless, the sum of these water energies in inherent structure number 6, the predecessor of the ACTS, possesses a minimum, which may indicate the initiation of ACTS.

Further investigation of possible driving forces, which cause the substrate to go into the transition state, leads, to a comparison of geometries (Figure 5a,b) and energies (Figure 5c) per residue between inherent structures 6 and 3 and the ACTS. The substrate contributions at position 105 (Figure 5b,c) repeat the geometrical and energetical differences already mentioned in Figures 3 and 4 and Table 4. We concentrated on continuous bars in Figure 5, because for a strained ACTS, which is expected to relax into any of the inherent structures via specific global degrees of freedom, we should find similar differences for both neighboring inherent structures. In the investigation of main chain dihedrals (Figure 5a), we find continuous bars for Asn36 and Gly94. These residues are part of two turns which are both

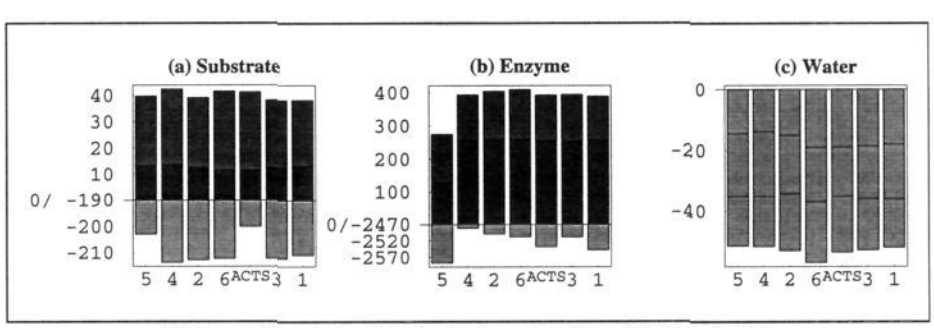

Figure 4. (a) Energy of the substrate, (b) energy of the enzyme, and (c) energy of three water molecules at the catalytic site. In (a) and (b) we have shaded the contributions of bond length, bond angle, and dihedral angle as well as the total energy in gray levels from dark to bright (different scale for positive and negative energies). In (c) the energies of all three water molecules at the catalytic site are summed into one bar.

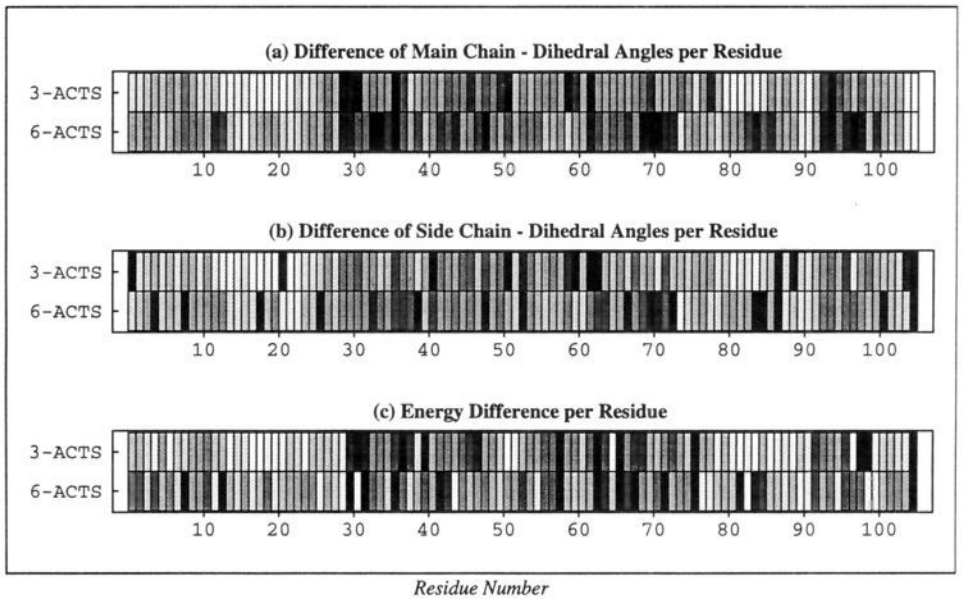

Figure 5. Comparison of the differences in the sum of the absolute values of (a) main chain dihedrals, (b) side chain dihedrals, and (c) total energies per residue between inherent structures 6 and 3 and the active conformational transition state (ACTS). Large differences are marked with dark fields.

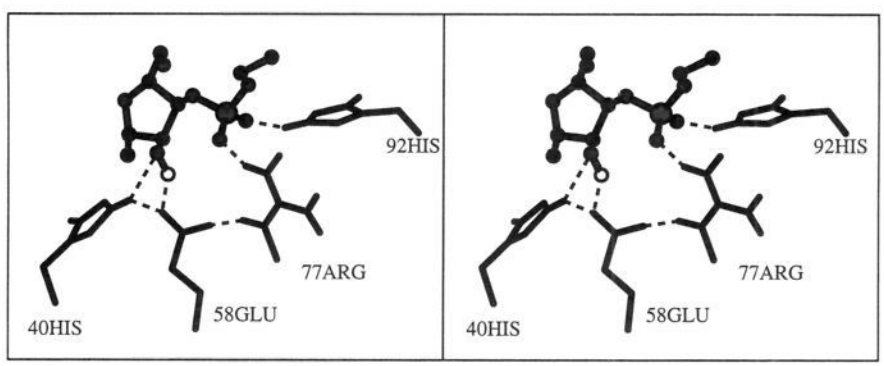

Figure 6. Conformation of the catlytic site of a possible initial state of the RNase T1 reaction. Only the ribose and phosphate group of the substrate and the side chains His40, Glu58, Arg77, and His92 are shown.

connected to the two active site histidines via hydrogen bonds Asn36 O···His40 Nδ1 and Ala95 N···His92 O.

In the side chain part (Figure 5b) the pattern is more diffuse. Only conformational changes for Ser53 and Ala87 occur in both transitions. A detailed graphical investigation shows for Ala87 a dihedral rotation from one minimum to the next with no influence on the structure. Ser53 on the other hand is totally solvent accessible, and therefore a rotation of the side chain dihedral is highly probable. A similar diffuse picture can be found for the energy differences per residue (Figure 5c). Besides the clear energy transition of the substrate on one side and Glu58 on the other, we find weaker transitions for Ser63, Asp66, and Asp76. Since these are one polar side chain and two charged side chains, these energy transitions can be expected to result from electrostatic reorientation due to the formation of ACTS.

Discussion

The conformation of the catalytic site in ACTS and the most important interactions between the enzyme and substrate are shown in Figure 6. The positive charges of $His40^+$ and $Arg77^+$ stabilize the negatively charged phophate and $Glu58^-$ groups, and there is a strong hydrogen bond between $His92^+$ and one of the anionic oxygens. The correspondence between our results and the known mechanistic proposals concerning the RNase T1 enzymatic activity[2,3] is obvious. All four amino acids brought to the nearest vicinity of the substrate by our simulation are within the scope of the conventional reaction mechanism.

Concerning the disputable role of the $His40^+/Glu58^-$ pair,[3] we have chosen $Glu58^-$ to play the role of the general base, justified by NMR titrations,[25] pH-dependent kinetic studies,[12] the stereochemistry of X-ray structures of the enzyme−product complex,[15] and independent Monte Carlo calculations (manuscript in preparation), which show a clear tendency for His40 and Glu58 to be charged during binding of a substrate. Moreover, our quantum-chemical results (Table 3) indicate that $Glu58^-$ can fit the role of the general base, because it induces a significant polarization and bond weakening in the C2′−O2′−HO2′ group, which could initiate the first proton transfer of the reaction. Steyaert et al.[12] argue in accordance with the earlier proposal of Nishikawa et al.[11] that this conventional mechanism can be replaced by a mechanism in which the deprotonated His40 plays the role of the general base, if and only if $Glu58^-$ is replaced by an electroneutral residue. But to prove this pathway, further simulations with the corresponding $Glu58^-$ mutated enzymes are required. Regarding the indication that $His40^+$ is involved in the catalytic activity of wild-type RNase T1, the found conformation of ACTS suggests that $His40^+$ regulates the arrangement of the general base $Glu58^-$ and the negatively charged target phosphate with respect to each other.

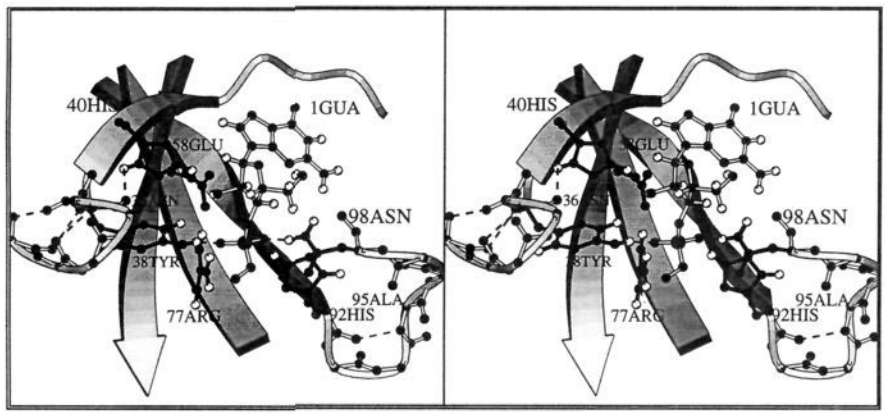

Figure 7. Hydrogen bond (dashed lines) connectivity of two loop regions around Asn36 and Gly94 with the active site histidines and of the side chains Tyr38 and Asn98 in the vicinity of these loops with the phosphoryl oxygens. Only the part of the substrate which belongs to the recognition and catalytic site is drawn.

A stabilizing role in the reaction pathway can be derived also for $Arg77^+$ from the conformation of ACTS. Interestingly, it was found from NMR and neutron diffraction data on a RNase A + uridine vanadate (VO5) complex (see references in ref 29) that $Lys41^+$ forms no hydrogen bonds with VO5, the stable analogue of the pentacoordinated phosphorus (phosphorane) transition state. Therefore, it could be called into question whether $Arg77^+$ in Rnase T1, which is the counterpart of $Lys41^+$ in RNase A, is involved in enzymatic activity. In addition ab initio quantum chemical calculations on the phosphorane and vanadate entities[29] have shown that, although the electrostatic potential and gross atomic populations agree well for the PO5 and VO5 residues, the P−O bonds are much more ionic than the V−O bonds. As a consequence, the pattern of $Lys41^+$ and His12 residue bonding in the uridine vanadate-inhibited RNase A is not recommended to be used in mechanistic studies,[29] and the hydrogen bridge as found in ACTS is possible.

The pH optimum of RNase T1 activity (~6) is far below the pK of $Arg77^+$, ~11, and is different from the pK of $His40^+$, <8.5.[25] Indeed, at pH 6, both $Arg77^+$ and $His40^+$ cannot participate in proton transfer. Because the probability of proton delocalization is higher for $His40^+$ than for $Arg77^+$, we believe that the histidine is a better candidate to electrostatically shield and mechanically regulate the general base $Glu58^-$, whereas $Arg77^+$ is essential for binding and orienting the target phophate in a correct geometry.

Another important point in the debate of the catalytic mechanism is the attack of the general acid on the substrate within the RNase T1 active site. Our MD simulation suggests that $His92^+$ as the general acid is strongly hydrogen bonded to O1P phosphate anionic oxygen. Interestingly, there is a striking parallel between our study and that on RNase A + cytidylyl-3′,5′-adenosine (CpA)[7] (20 ps simulation with the CHARMM force field). This study and our own contradict the conventional belief[1−3] that $His92^+$ in RNase T1 and $His119^+$ in RNase A are hydrogen-bonded directly to the O5′ esteric oxygen of the phosphate at the beginning of the reaction. Both MD results are in full agreement with the recent proposal by Anslyn and Breslow.[16] Since the Anslyn−Breslow publication as a whole was criticized in the literature,[17] our CNDO/2-spd results might help to clarify this point. First, Table 3 shows that the phosphate anionic oxygens in the isolated $GpCH_3$ are much richer in electron density than the esteric ones, and therefore, they should be better hydrogen bond acceptors. Further, independent calculations show that a mere hydrogen bond of $His92^+$ to O1P phosphate anionic oxygen results in a noticeable polarization of the C2′−O2′−HO2′ group of the ribose. This agrees well with both the conventional mechanism[1−3] and that proposed by Anslyn and Breslow.[16] Specifically, such a polarized C2′−O2′−HO2′ group is now better adjusted to donate its proton to any kind of general base.

It should be noted in this context that the very recent mechanistic proposal by Lim and Tole[30] calls into question the conventionally recognized proton transfers from the general acid to the phosphate and from O2′−HO2′ to the general base. On the basis of detailed ab initio calculations on the model reaction, Lim and Tole propose that, in RNase A, $His119^+$ merely hydrogen bonds to the phosphoryl oxygen, whereas His12 facilitates the intramolecular transfer of the 2′-hydroxyl oxygen to a phosphoryl oxygen (tautomeric conversion). Such a mechanism applied to RNase T1 reduces the functional roles of all side chains except for the general base. This proposal is not in accordance with our quantum-chemical results (Table 3), where we have found for inherent structures 6 and 3, which possess an intramolecular hydrogen bond between the 2′-hydroxyl group and the phosphoryl oxygen, a lower polarization of the hydroxyl group compared with ACTS. Moreover, this mechanism seems to contradict recent kinetic studies on double mutants of RNase T1[31] which showed cooperativity and a nonadditivity of the functional interactions between His40 and Glu58, Glu58 and His92, and His40 and His92.

The functional interplay of the two histidines is also supported by our extraction of possible global degrees of freedom, which could be responsible for the strained conformation of the ACTS (Figure 5). The observed main chain transitions in the loop regions around Asn36 and Gly94 are connected via hydrogen bonds with the side chain of His40 and the main chain of His92 (Figure 7). The influence of His92 on the structural flexibility of the loop 91−101 was also indicated in the X-ray structure of the inactive His92Ala mutant,[32] but cannot be explained merely by the formation of a main chain hydrogen bond His92 N···Ala95 O, which was found in ACTS. The vicinity of the mentioned loops is connected with the substrate via hydrogen bonds of Tyr38 Oη and Asn98 Nδ2 to the two phosphoryl oxygens (Figure 7). A strong correlation of Tyr38 and Asn98 via the phosphate group is in accordance with biochemical experiments,[33] which have shown a nonadditive influence of these side chains on the turnover of the reaction. This work[33]

(29) Krauss, M.; Basch, H. *J. Am. Chem. Soc.* **1992**, *114*, 3630−3634.
(30) Lim, C.; Tole, P. *J. Am. Chem. Soc.* **1992**, *114*, 7245−7252.
(31) Steyaert, J.; Wyns, L. *J. Mol. Biol.* **1993**, *229*, 770−781.
(32) Koellner, G.; Choe, H.-W.; Heinemann, U.; Grunert, H.-P.; Zouni, A.; Hahn, U.; Saenger, W. *J. Mol. Biol.* **1992**, *224*, 701−713.
(33) Steyaert, J.; Haikal, A. F.; Wyns, L. *Proteins* **1994**, *18*, 318−328.

is in accordance with other results on RNase T1 mutants in active site residues as His40, Glu58, and His92, which have shown contributions of these residues to chemical turnover but only minor effects on substrate binding. On the first glance, these experimental data seem to contradict our results, which show all the mentioned residues in hydrogen bond contacts with the 2′-hydroxyl and phosphate group of the substrate (Table 4). The reason for this apparent contradiction lies in the inability of MD methods to simulate chemical reactions. All the hydrogen bonds mentioned above involve the chemically reactive part of the substrate, and at least some of them will change or break when the transesterification starts. This argument is obvious for the role of the general base and acid, but also holds for the hydrogen bonds to the phosphate group, which will be reorientated in the first step of the reaction. We conclude that the hydrogen bonds in the active site perform a kinetic control of the reaction. First, they enable the proton transfer to and from the substrate, and second, they direct the enzyme's global degrees of freedom onto the substrate and force it into a strained conformation. Therefore, these hydrogen bonds should have only short lifetimes and minor influence on the binding constants.

A detailed investigation of the effects of global conformational changes on catalytic activity has to be postponed to further longer dynamical simulations.

Acknowledgment. This work was supported by the Deutsche Forschungsgemeinschaft through Schwerpunktprogramm "Protein Design", a grant to E.B.S., and by Fonds der Chemischen Industrie.

JA951302H